

Gauged Lepton Number and Cosmic-ray Boosted Dark Matter for the XENON1T Excess

Yongsoo Jho,^{1,*} Jong-Chul Park,^{2,†} Seong Chan Park,^{1,‡} and Po-Yan Tseng^{1,§}

¹*Department of Physics and IPAP, Yonsei University,
Seoul 03722, Republic of Korea*

²*Department of Physics, Chungnam National University, Daejeon 34134, Republic of Korea*

Abstract

The recently reported excess in XENON1T is explained by two scenarios with and without a dark matter interaction with the gauged lepton number, $U(1)_{L_e-L_i}$, $i = \mu$ or τ . In Scenario#1, the gauge boson provides non-standard interaction between solar neutrino and electron that enhances the number of electron recoil events in the XENON1T detector. In Scenario#2 with the gauge coupling to dark matter, dark matter can be boosted by cosmic electrons and generate electron recoil energy up to $\mathcal{O}(\text{keV})$ to explain the XENON1T result. The dark matter, aided by the new gauge interaction, could heat up a neutron star more than 1500 K as a neutron star captures the halo dark matter. Therefore, we propose to utilize the future infrared telescope to test our scenario.

* jys34@yonsei.ac.kr

† jcpark@cnu.ac.kr

‡ sc.park@yonsei.ac.kr

§ tpoyan1209@gmail.com

I. INTRODUCTION

An excess in low energy electronic recoil events over known backgrounds has been reported by the XENON1T collaboration [1]. The excess is rising towards lower energies below 7 keV and most prominent in 2-3 keV, which may be simply due to the Tritium contamination. New particles beyond the standard model (SM) such as solar axions, solar neutrinos, light axion-like-particles (ALPs), and dark photon dark matter have been proposed to explain the excess by the XENON1T collaboration [1], but none of them is favored by experimental and observational data [2–8]. The XENON1T result prefers the electron recoil spectrum by boosted dark matter (DM) [9], and there exist various suggested mechanisms, for example by cosmic-ray [10, 11], Sun [12], decay or annihilation [13, 14] of heavier particles. It can also be explained by non-standard neutrino-electron interactions coming from the neutrino magnetic moment [15] or by dark photon [16–20]. Inelastic DM scenarios are discussed in Refs. [21, 22]. In addition, Migdal effect[23] and solar axion[24] have been studied.

In this work, we focus on two other possibilities: i) the non-standard neutrino-electron interaction via an exchange of a light gauge boson X and ii) boosted DM upscattered by the cosmic-ray electrons. Both possibilities can be realized under a signal framework by introducing a gauge boson mediator which couples to both electronic and dark matter sectors. We take the differences in family-lepton numbers, $L_e - L_\mu$ or $L_e - L_\tau$, as the new gauge symmetry [25] and propose two scenarios for definiteness:

- Scenario#1: The solar neutrinos can interact with electrons in the XENON1T detector by the exchange of the new gauge boson, X_μ , and generate signals [26].
- Scenario#2: The dark matter couples with the new gauge boson as well. The up-scattered DM particles by cosmic-ray electrons and neutrinos [27, 28] in addition to solar neutrinos can interact with electrons in the XENON1T detector and produce the observed excessive signals.

One should note that our choice is theoretically well motivated as the new gauge interactions are anomaly-free.¹

With the gauged symmetry $U(1)_{L_e-L_i}$ with $i = \mu$ or τ , the Lagrangian includes the interactions of the new gauge boson, X_μ , with electron, neutrino, and also DM:

$$\mathcal{L}_{Scen\#1} \supset -g_e X_\mu (J_e^\mu + J_\nu^\mu) + \dots, \quad (1)$$

$$\mathcal{L}_{Scen\#2} \supset \mathcal{L}_{Scen\#1} + g_\chi X_\mu J_\chi^\mu, \quad (2)$$

where “...” include the kinetic terms and also interactions with other leptons. The dark matter interaction is allowed only in Scenario#2. The vector currents are given by

$$J_\psi = \bar{\psi} \gamma^\mu \psi \quad \text{where} \quad \psi = e, \mu, \dots, \chi. \quad (3)$$

¹ In general, the gauge symmetries of lepton numbers and baryon numbers in the form $(L_i - L_j) + \epsilon(B_k - L_k)$ with various combinations of different generations $(i, j, k, = 1, 2, 3)$ are anomaly free [29]. Also see [30] for the recent J-PARC KOTO anomaly.

II. SCENARIO#1

In Scenario#1, we consider the electron recoil spectrum from the non-standard scattering between the solar neutrino and the electron in the XENON1T detector via the exchange of a X boson. The solar neutrinos are produced by main processes of solar nuclear reaction chains [31]. In the range of keV-MeV, these processes can generate sizeable amount of neutrinos which can affect in this scenario. The recoil energy spectrum is given by

$$\frac{dR^X}{dE_r} = N_T \cdot \epsilon(E_r) \cdot \int_{E_\nu^{\min}(E_r)}^{\infty} \frac{d\Phi_{\text{solar } \nu}}{dE_\nu} \frac{d\sigma_{\nu e}^X}{dE_r} dE_\nu, \quad (4)$$

where E_ν is the energy of the solar neutrino, $\epsilon(E_r)$ is the efficiency of electron recoil in the XENON1T detector. In the presence of a new leptophilic $U(1)_{L_e-L_i}$ gauge boson X , coupled to both electron and neutrinos, the differential cross section of neutrino-electron scattering $\nu e^- \rightarrow \nu e^-$ is given by

$$\frac{d\sigma_{\nu e}^X}{dE_r} = \frac{(g_e g_\nu)^2 m_e}{4\pi p_\nu^2 (m_X^2 + 2E_r m_e)^2} [2E_\nu^2 + E_r^2 - 2E_\nu E_r - E_r m_e - m_\nu^2]. \quad (5)$$

Here for a given recoil energy E_r , the minimum value of the neutrino energy is given by

$$E_\nu^{\min} = \frac{1}{2} \left(E_r + \sqrt{E_r^2 + 2E_r m_e} \right), \quad (6)$$

N_T is the total number of the target electrons in the XENON1T detector. We perform the χ^2 minimization for electron recoil spectrum dR/dE_r by summing up the background and new physics contributions. The favored region is shown in Fig. 1.

However, the X boson in the parameter region favored by the XENON1T excess can speed up the cooling process of the Sun and Globular clusters significantly. Because the X boson with $m_X \simeq 100$ keV can be copiously produced by thermal radiation of electrons and the solar plasmon resonance. If the coupling g_e of X is small enough, X can escape from the Sun and contribute extra cooling, which is constrained as ‘‘Stellar Cooling’’. Even if, the mass of X is outside the plasmon resonance region, neutrinos still can be produced through an off-shell X and escape the Sun. This process provides another constrained region, the so-called ‘‘Cooling via ν emission’’. If the coupling is large enough, i.e $g_e \gtrsim 4 \times 10^{-7}$, the X boson cannot escape the Sun. However, its decay into neutrinos still contributes to the cooling, thus the relevant parameter region is excluded and called ‘‘Cooling via ν emission’’. We also show other constraints on Scenario#1 with $U(1)_{L_e-L_{i=\mu,\tau}}$. For more details, see Section IV.

III. SCENARIO#2

In this section, we consider two possibility of the DM and electron interactions, one is simply used the effective DM-electron cross section $\sigma_{\text{DM-e}}$, and the other comes from

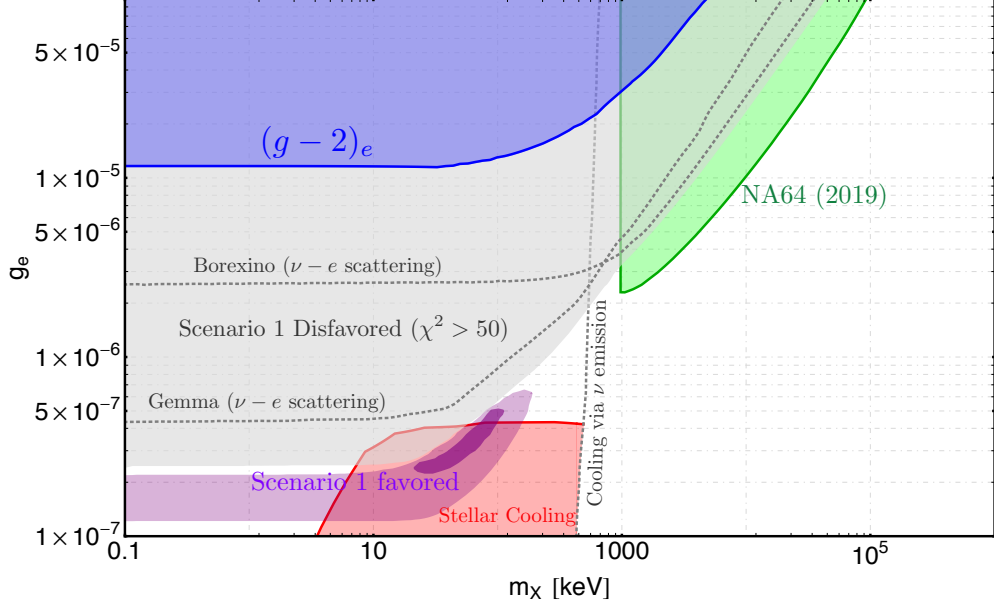


FIG. 1: The favored and disfavored regions in Scenario#1. The dark purple and light purple regions are favored by XENON1T by χ^2 minimization. The gray shaded region is disfavored as $\chi^2 > 50$. The constraints on electron coupling g_e from $(g-2)_e$ (blue), the cooling of the Sun and Gloubular clusters (red) and the missing momentum search for invisibly decaying dark photon by NA64 experiment (green) are also shown. The gray dotted lines are the constraints in the presence of g_e and g_ν , from ν - e scattering (Borexino, Gemma) and the stellar cooling by neutrino emission.

exchanging of the X gauge boson as describe in Eq.(2). For the later case, we adopt the differential cross section for $\text{DMe} \rightarrow \text{DMe}$ as function of the recoil energy [26]

$$\frac{d\sigma_X(\text{DMe} \rightarrow \text{DMe})}{dE_e} = \frac{(g_e g_\chi)^2 m_e}{4\pi p_{\text{DM}}^2 (m_X^2 + 2E_e m_e)^2} [2E_{\text{DM}}^2 + E_e^2 - 2E_{\text{DM}} E_e - E_e m_e - m_{\text{DM}}^2], \quad (7)$$

where E_{DM} and E_e is the DM energy and the recoil energy transferred to the target electron. The maximal recoil energy is given by

$$E_e^{\text{max}}(E_{\text{DM}}) = \frac{2m_e(E_{\text{DM}}^2 + 2m_{\text{DM}} E_{\text{DM}})}{(m_{\text{DM}} + m_e)^2 + 2m_e E_{\text{DM}}}.$$

Due to the DM-electron interactions, the non-relativistic halo DM will be boosted by high energy electron cosmic-ray $d\Phi_e/d\Omega$, which is from observations of Voyager, AMS-02, DAMPE, and Fermi-LAT between $2\text{MeV} \leq E_e \leq 90\text{GeV}$ [32]. The boosted DM flux can be obtained by convolution of the electron flux and DM-electron differential cross section[28]

$$\frac{d\Phi_{\text{DM}}}{d\Omega}(E_{\text{DM}}, b, l) = \frac{J(b, l)}{m_{\text{DM}}} \int dE_e \frac{d\Phi_e}{d\Omega} \frac{d\sigma_{\text{DMe} \rightarrow \text{DMe}}}{dE_{\text{DM}}}, \quad (8)$$

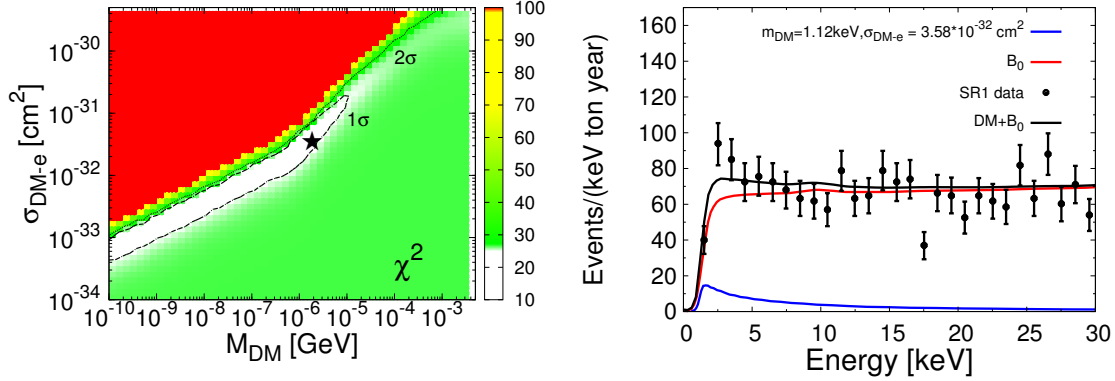


FIG. 2: Left-panel: The χ^2 distribution in the plane of $(m_{\text{DM}}, \sigma_{\text{DM-e}})$ by fitting to the event spectrum from XENON1T. The best-fit point gives $\chi^2_{\text{best-fit}} = 22.74$ labelled with the “star” symbol, where the curve B_0 gives $\chi^2_{B_0} = 26.56$. The 1σ and 2σ regions correspond to $\Delta\chi^2 \equiv \chi^2 - \chi^2_{\text{best-fit}} = 2.30, 5.99$, respectively. Right-panel: The event spectrum for the best-fit point.

where $J(b, l) = \int_{l.o.s} d\ell \rho_{\text{DM}}$ is the line of sight integral of the DM energy density ρ_{DM} in the direction of galactic coordinates (b, l) . For effective cross section case, we replace the differential cross section $d\sigma_{\text{DM}e \rightarrow \text{DM}e}/dE_{\text{DM}}$ by $\sigma_{\text{DM-e}}/E_{\text{DM}}^{\text{max}}(E_e)$. Then we use the boosted DM flux to compute the electron recoil energy spectrum for XENON1T.

The χ^2 fitting results of the effective cross section case are shown in Fig.2. The best-fit value $(m_{\text{DM}}, \sigma_{\text{DM-e}}) = (1.12 \text{ keV}, 3.58 \times 10^{-32} \text{ cm}^2)$ gives $\chi^2_{\text{best-fit}} = 22.74$, which slightly improves the SM result of $\chi^2_{B_0} = 26.56$. The left-panel shows the 1σ and 2σ contours. The XENON1T prefers $m_{\text{DM}} \lesssim 10$ keV, and linear correlation between $\sigma_{\text{DM-e}}$ and m_{DM} . Since the Event rate is proportional to the square of $\sigma_{\text{DM-e}}$, the upper-left corner (red region) overproduces the events is ruled out by XENON1T results. The “star” labels the best-fit point, and its spectrum is shown in the right-panel and features a peak around 2 – 3 keV.

For the X gauge boson mediator case, there are three independent parameters $(m_{\text{DM}}, m_X, g_e g_X)$ are relevant to produce electric recoil spectrum for XENON1T. The spectra shapes depend on the m_X are shown in Fig.3 with $m_X = 0.4, 1, 10, 100$ MeV. And XENON1T data prefers $m_X \lesssim 10$ MeV in order to feature a peak around 2 – 3 keV. In Fig.4, the spectrum is not sensitive to DM mass within the range $0.01 \text{ keV} < m_{\text{DM}} < 100 \text{ keV}$. The χ^2 distribution from scanning the three parameters $(m_{\text{DM}}, m_X, g_e g_X)$ are exhibited in Fig.5. The m_X lighter than 4 MeV and linear correlation between $\sqrt{g_e g_X}$ and m_X are preferred by the ZENON1T data. The red regions over producing the events are excluded by XENON1T results. The minimal χ^2 point, $(m_{\text{DM}}, m_X, \sqrt{g_e g_X}) = (1.45 \text{ keV}, 0.41 \text{ MeV}, 7.15 \times 10^{-3})$, labelled with “star” gives $\chi^2_{\text{best-fit}} = 22.47$ and yields the event spectrum in bottom-right panel of Fig.5.

We show the current constraints on the mediator’s electron coupling and mass in Scenario#2 in Fig. 6 by fixing $g_X = 3.0$ and $g_\nu = 0$, therefore, the neutrino experiments and stellar cooling through neutrino are not relevant. Further more, missing E_T searches via

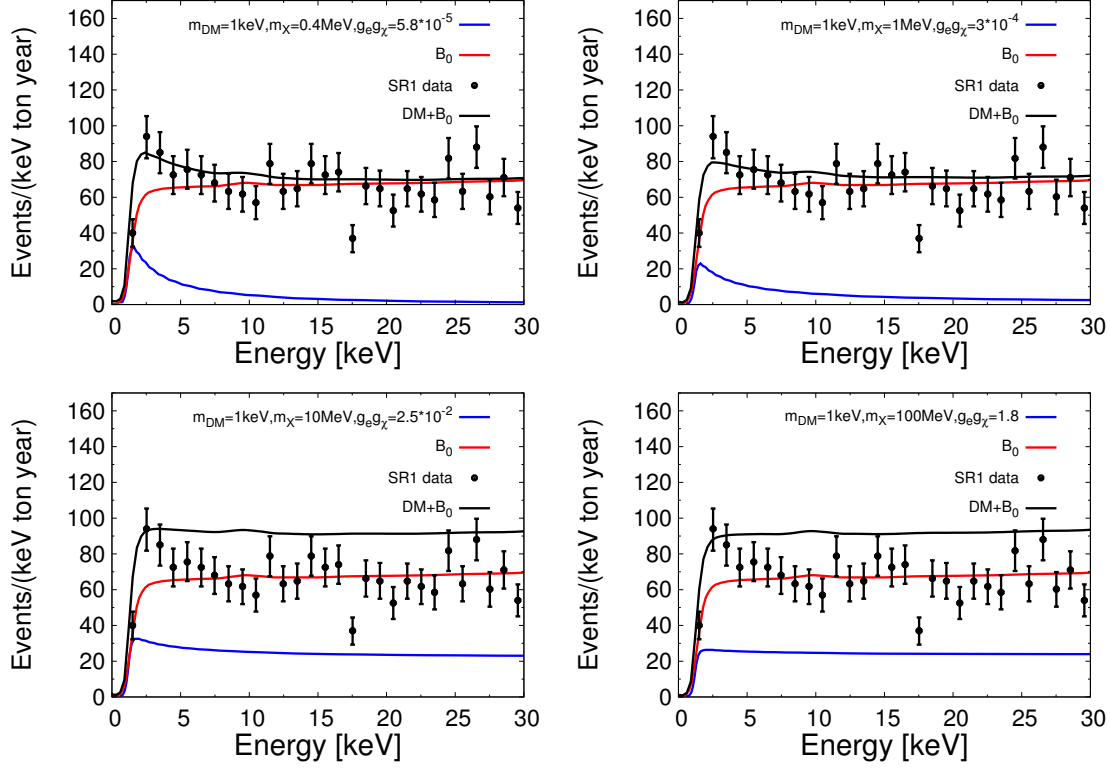


FIG. 3: The event spectra for the XENON1T with respect to $m_X = 0.4, 1, 10, 100$ MeV.

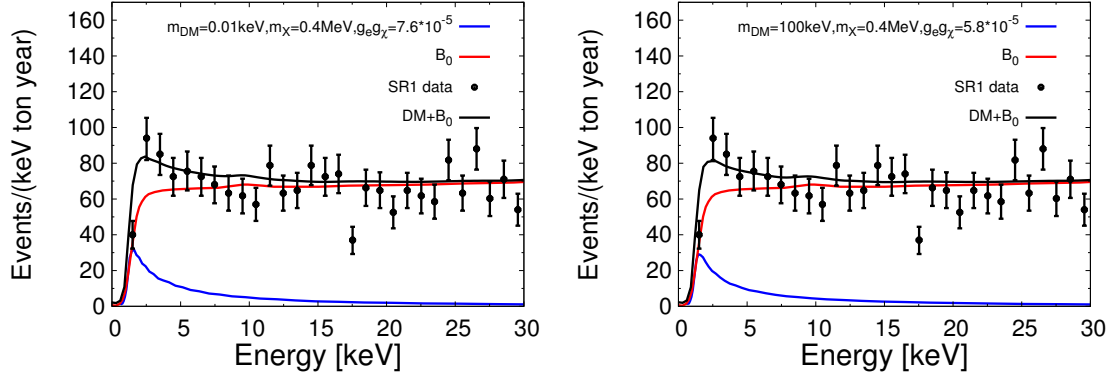


FIG. 4: The event spectra for the XENON1T with respect to $m_{DM} = 0.01, 100$ keV.

invisible decay of dark gauge boson from NA64 shows no constraints for the mass below some values because they can just measure missing E_T within their detection resolution. So, for too light dark boson ($m_X < E_{\text{resolution}}$), they cannot provide any constraints. Consequently, the XENON1T preferred 1σ region is shown by purple color is still allowed and consistent with present observations. See Sec.IV for other constraints. Finally, for the test of Scenario#2, we would like to discuss the heating of neutron star from capturing the halo DM in Section V.

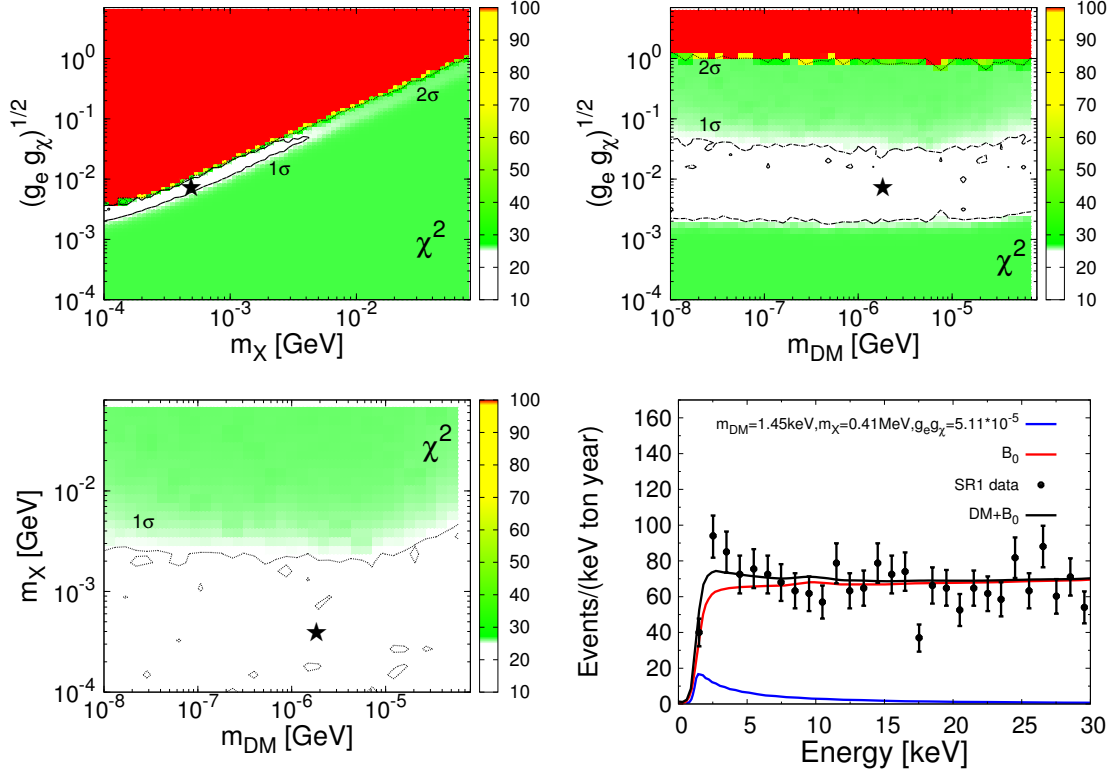


FIG. 5: For Scenario#2, the χ^2 scanning of $(m_{\text{DM}}, m_X, \sqrt{g_e g_\chi})$ project to $(m_X, \sqrt{g_e g_\chi})$, $(m_{\text{DM}}, \sqrt{g_e g_\chi})$, and (m_{DM}, m_X) planes. Bottom-Right panel: The event spectrum of the best-fit point $(m_{\text{DM}}, m_X, \sqrt{g_e g_\chi}) = (1.45 \text{ keV}, 0.41 \text{ MeV}, 7.15 \times 10^{-3})$ with $\chi^2_{\text{Best-fit}} = 22.47$.

IV. CONSTRAINTS FROM OTHERS

The model in Scenario #1 and Scenario #2 can be probed by various searches as follows:

- $(g-2)_e$: The anomalous magnetic moment of electron, $(g-2)_e$ can be enhanced due to the one-loop correction including light X boson. For, $m_X \ll m_e$, a sizeable coupling $g_e \gtrsim 10^{-5}$ is constrained.
- *Invisibly decaying dark photon search in NA64 experiment*: For $m_X \gtrsim 1 \text{ MeV}$, a large X boson coupling to electron as $g_e \gtrsim 10^{-5} - 10^{-6}$ has been probed by the dark photon search at NA64 experiment [33].
- *Stellar cooling constraints*: If X boson in the mass range $m_X \in [10^2, 10^5] \text{ eV}$ is weakly coupled to the electron as $g_e \in [10^{-12}, 10^{-7}]$, X boson can be produced inside the Sun and easily escape the Sun due to its long lifetime [34]. In the absence of the neutrino coupling, X boson with the coupling $g_e \gtrsim 10^{-7}$ is still allowed because it is captured by the Sun before the escape. In the presence of neutrino coupling g_ν , the produced X boson predominantly decays into neutrino pair. The escape of these neutrino pairs

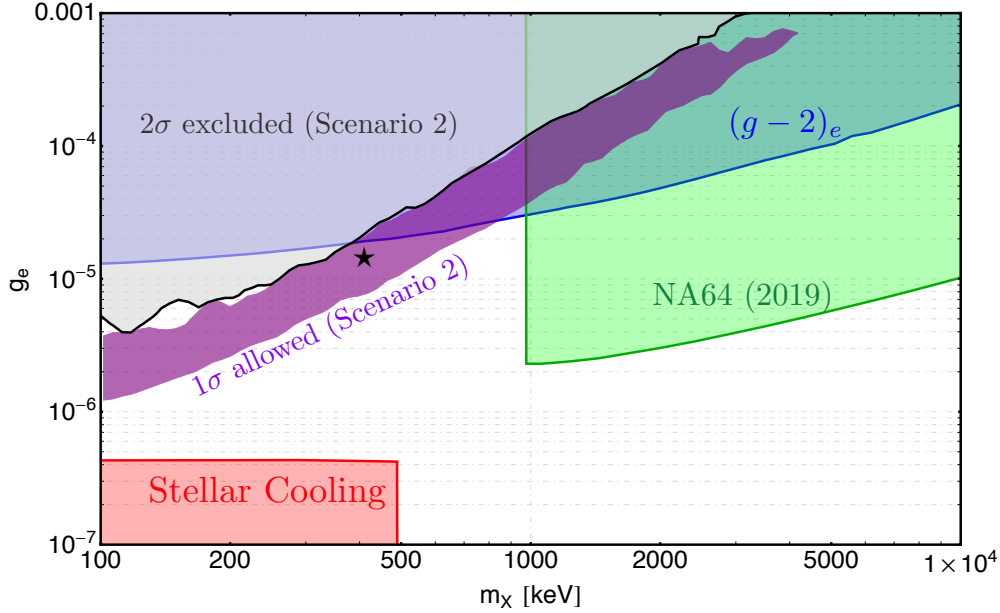


FIG. 6: The favored (purple) and disfavored (gray) regions of the parameters (m_X, g_e) in Scenario#2 with $g_\chi = 3.0$ and $g_\nu = 0$. The constraints on g_e from $(g - 2)_e$ (blue), stellar cooling (red), and NA64 (green) are also shown. The “star” marker indicates the same benchmark point as in Fig. 5.

from stellar object will significantly increase the rate of cooling, even with the larger coupling value $g_\nu \gtrsim 10^{-7}$ [35].

- *Neutrino-electron scattering:* Borexino [36] and Gemma [37] provide the limit of non-standard neutrino interaction by measuring ν - e^- scattering cross section, using ^7Be solar neutrino and reactor neutrino, respectively. We show their limits in the case of $g_X = g_e = g_\nu$ in Fig. 1.

V. NEUTRON STAR HEATING

As an important prediction of our proposal in this paper is that a neutron star(NS) can be heated up to 1500 K by capturing DM particles in halo and this will get tested by near future infrared telescope, for example the James Webb Space Telescope [38].

The halo DM couples to electron can be captured by 5% electron component inside the neutron star(NS)[39], and heats up NS due to the acceleration by the strong NS gravity. After been captured, the DM kinematic energy transfers to the NS heat energy. Even through, the DM is leptophilic, if the DM-electron cross section is large enough, the NS capture rate can be greater than geometric limit[40]² and such that the DM can heat up

² The geometric limit means the whole halo DM around NS are all the captured. The geometric limit of

the NS and increase the NS temperature by 1500 K [41]. The deviation from the $\mathcal{O}(10^8)$ years old NS temperature evolution by $\mathcal{O}(1000)$ K will be sensitive to near future infrared telescope.

The approximating capture rate by electron component of NS is [42]

$$C_c \simeq \sqrt{\frac{6}{\pi}} \frac{\rho_{\text{DM}}}{m_{\text{DM}}} \frac{v_{\text{esc}}^2(R_{\text{NS}})}{\bar{v}^2} (\bar{v}\xi) N_e \int dE_e \frac{d\sigma_X(\text{DMe} \rightarrow \text{DMe})}{dE_e}, \quad (10)$$

which includes the Pauli blocking suppression factor $\xi \equiv \delta p/p_F$ where δp is typical momentum transfer, and p_F is the Fermi momentum [42], where $p_F \simeq 200$ MeV [39] and $\delta p \simeq \mathcal{O}(\text{keV})$ for $m_{\text{DM}} \simeq \mathcal{O}(\text{keV})$. Therefore, the Pauli blocking gives a suppression factor of $\xi \simeq \mathcal{O}(10^{-5} - 10^{-6})$ for keV DM. The escape velocity of the NS is $v_{\text{esc}}(R_{\text{NS}}) = \sqrt{2GM_{\text{NS}}/R_{\text{NS}}} \simeq 0.63c$, \bar{v} is the DM dispersion velocity, and ρ_{DM} is the local DM density, and N_e is the total number of electrons in the NS.

For the effective DM-electron cross section from Fig.2, the best-fit point gives $\xi\sigma_{\text{DM-e}} \simeq \mathcal{O}(10^{-37} - 10^{-38})$, which is much larger than the critical cross section $\sigma_{\text{DM-e}}|_{\text{crit}} \simeq 5 \times 10^{-44} \text{ cm}^2$. Therefore, the best-fit point and the entire region preferred by XENON1T will be probed by the NS heating process and near future infrared observations. For the X boson mediator case, substitute the best-fit value from Fig.5 into Eq.(10), it yields the capture rate $C_c \simeq 6.7 \times 10^{34} \text{ sec}^{-1}$, that is much larger than the geometric limit $C|_{\text{geom}} \simeq 1.5 \times 10^{31} \text{ sec}^{-1}$, result in heating up the NS by 1500 K.

VI. CONCLUSION

In this paper, we discuss the explanation of recent XENON1T electron recoil spectrum excess around 2 – 3 keV. We consider a leptophilic vector mediator coupled to leptons and keV-MeV dark matter in two specific scenarios.

First, in Scenario#1, we check that the solar neutrino and target electron in XENON1T can generate the low-recoil energy excess very well, in the presence of light mediator coupled to both electrons and neutrinos, with $m_X \sim 10 - 100$ keV mass and $g_e = g_\nu \sim (3 - 4) \times 10^{-7}$, although the stellar cooling and neutrino-electron scattering constraints are stringent at the favored region.

Second, in Scenario#2, we find the possibility to explain the XENON1T recoil spectrum excess using the boosted light dark matter, upscattered by energetic electron cosmic rays. Firstly, we checked the effective DM-electron cross section case. Then we consider the gauge mediator X boson to realize the DM-electron interaction. Where the mediator mass $m_X \lesssim 4$ MeV is crucial to generate the peak around 2-3 keV in electron recoil spectrum, and thus

the NS capture rate is estimated by

$$C|_{\text{geom}} = 5.6 \times 10^{25} \left(\frac{\rho_X}{\text{GeV/cm}^3} \cdot \frac{1\text{GeV}}{m_{\text{DM}}} \cdot \frac{R_{\text{NS}}}{11.6\text{km}} \cdot \frac{M_{\text{NS}}}{1.52m_\odot} \right) \text{ s}^{-1}, \quad (9)$$

where R_{NS} , M_{NS} are the radius and mass of typical NS star, respectively. Or rough estimation gives the critical cross section between DM and electron, $\sigma_{\text{DM-e}}|_{\text{crit}} \simeq \pi R_{\text{NS}}^2/N_e \simeq 5 \times 10^{-44} \text{ cm}^2$.

preferred by XENON1T. In the 1σ region, the $\sqrt{g_e g_\chi}$ has strong correlation with m_χ , but the produced spectrum is not sensitive to DM mass in $0.01 \text{ keV} \lesssim m_{\text{DM}} \lesssim 100 \text{ keV}$. From the χ^2 minimization, $(m_{\text{DM}}, m_\chi, \sqrt{g_e g_\chi}) = (1.45 \text{ keV}, 0.41 \text{ MeV}, 7.15 \times 10^{-3})$ provides best-fit to the data. We also check the other direct constraints on the electron coupling g_e in the absence of the neutrino coupling ($g_\nu = 0$) in Scenario#2. Requiring a large coupling between the mediator and the dark matter $g_\chi \sim \mathcal{O}(1)$, we observe that the favored region of XENON1T is still allowed from the current constraints.

Finally, we emphasize that the observation of $\mathcal{O}(10^8)$ year old NS by near future infrared telescopes will probe the allowed parameter region, base on values of $(m_{\text{MD}}, m_\chi, \sqrt{g_e g_\chi})$ that the halo DM capturing process by the electron component of NS is able to increase the NS temperature more than 1500 K.

Acknowledgments— The work is supported in part by Basic Science Research Program through the National Research Foundation of Korea (NRF) funded by the Ministry of Education, Science and Technology (NRF-2018R1A4A1025334, NRF-2019R1A2C1089334 (SCP) and NRF-2019R1C1C1005073(JCP)).

-
- [1] XENON collaboration, E. Aprile et al., *Observation of Excess Electronic Recoil Events in XENON1T*, 2006.09721.
 - [2] N. Viaux, M. Catelan, P. B. Stetson, G. Raffelt, J. Redondo, A. A. R. Valcarce et al., *Neutrino and axion bounds from the globular cluster M5 (NGC 5904)*, *Phys. Rev. Lett.* **111** (2013) 231301, [1311.1669].
 - [3] A. Ayala, I. Domnguez, M. Giannotti, A. Mirizzi and O. Straniero, *Revisiting the bound on axion-photon coupling from Globular Clusters*, *Phys. Rev. Lett.* **113** (2014) 191302, [1406.6053].
 - [4] M. M. Miller Bertolami, B. E. Melendez, L. G. Althaus and J. Isern, *Revisiting the axion bounds from the Galactic white dwarf luminosity function*, *JCAP* **10** (2014) 069, [1406.7712].
 - [5] T. Battich, A. H. Cserico, L. G. Althaus, M. M. Miller Bertolami and M. Bertolami, *First axion bounds from a pulsating helium-rich white dwarf star*, *JCAP* **08** (2016) 062, [1605.07668].
 - [6] M. Giannotti, I. G. Irastorza, J. Redondo, A. Ringwald and K. Saikawa, *Stellar Recipes for Axion Hunters*, *JCAP* **10** (2017) 010, [1708.02111].
 - [7] A. H. Cserico, L. G. Althaus, M. M. Miller Bertolami, S. Kepler and E. Garca-Berro, *Constraining the neutrino magnetic dipole moment from white dwarf pulsations*, *JCAP* **08** (2014) 054, [1406.6034].
 - [8] S. A. Daz, K.-P. Schrder, K. Zuber, D. Jack and E. E. B. Barrios, *Constraint on the axion-electron coupling constant and the neutrino magnetic dipole moment by using the*

- tip- RGB luminosity of fifty globular clusters*, 1910.10568.
- [9] K. Kannike, M. Raidal, H. Veerme, A. Strumia and D. Teresi, *Dark Matter and the XENON1T electron recoil excess*, 2006.10735.
 - [10] R. Primulando, J. Julio and P. Uttayarat, *Collider Constraints on a Dark Matter Interpretation of the XENON1T Excess*, 2006.13161.
 - [11] Q.-H. Cao, R. Ding and Q.-F. Xiang, *Exploring for sub-MeV Boosted Dark Matter from Xenon Electron Direct Detection*, 2006.12767.
 - [12] Y. Chen, J. Shu, X. Xue, G. Yuan and Q. Yuan, *Sun Heated MeV-scale Dark Matter and the XENON1T Electron Recoil Excess*, 2006.12447.
 - [13] J. Buch, M. A. Buen-Abad, J. Fan and J. S. C. Leung, *Galactic Origin of Relativistic Bosons and XENON1T Excess*, 2006.12488.
 - [14] G. Choi, M. Suzuki and T. T. Yanagida, *XENON1T Anomaly and its Implication for Decaying Warm Dark Matter*, 2006.12348.
 - [15] A. N. Khan, *Can nonstandard neutrino interactions explain the XENON1T spectral excess?*, 2006.12887.
 - [16] K. Nakayama and Y. Tang, *Gravitational Production of Hidden Photon Dark Matter in light of the XENON1T Excess*, 2006.13159.
 - [17] D. Aristizabal Sierra, V. De Romeri, L. J. Flores and D. K. Papoulias, *Light vector mediators facing XENON1T data*, 2006.12457.
 - [18] M. Du, J. Liang, Z. Liu, V. Q. Tran and Y. Xue, *On-shell mediator dark matter models and the Xenon1T anomaly*, 2006.11949.
 - [19] G. Alonso-lvarez, F. Ertas, J. Jaeckel, F. Kahlhoefer and L. J. Thormaehlen, *Hidden Photon Dark Matter in the Light of XENON1T and Stellar Cooling*, 2006.11243.
 - [20] C. Boehm, D. G. Cerdeno, M. Fairbairn, P. A. N. Machado and A. C. Vincent, *Light new physics in XENON1T*, 2006.11250.
 - [21] N. F. Bell, J. B. Dent, B. Dutta, S. Ghosh, J. Kumar and J. L. Newstead, *Explaining the XENON1T excess with Luminous Dark Matter*, 2006.12461.
 - [22] G. Paz, A. A. Petrov, M. Tammaro and J. Zupan, *Shining dark matter in Xenon1T*, 2006.12462.
 - [23] U. K. Dey, T. N. Maity and T. S. Ray, *Prospects of Migdal Effect in the Explanation of XENON1T Electron Recoil Excess*, 2006.12529.
 - [24] L. Di Luzio, M. Fedele, M. Giannotti, F. Mescia and E. Nardi, *Solar axions cannot explain the XENON1T excess*, 2006.12487.
 - [25] X.-G. He, G. C. Joshi, H. Lew and R. R. Volkas, *Simplest Z-prime model*, *Phys. Rev. D* **44** (1991) 2118–2132.
 - [26] R. Harnik, J. Kopp and P. A. Machado, *Exploring $\nu\bar{\nu}$ Signals in Dark Matter Detectors*, *JCAP* **07** (2012) 026, [1202.6073].
 - [27] T. Bringmann and M. Pospelov, *Novel direct detection constraints on light dark matter*,

- Phys. Rev. Lett.* **122** (2019) 171801, [1810.10543].
- [28] Y. Ema, F. Sala and R. Sato, *Light Dark Matter at Neutrino Experiments*, *Phys. Rev. Lett.* **122** (2019) 181802, [1811.00520].
 - [29] M. Bauer, P. Foldenauer and J. Jaeckel, *Hunting All the Hidden Photons*, *JHEP* **18** (2020) 094, [1803.05466].
 - [30] Y. Jho, S. M. Lee, S. C. Park, Y. Park and P.-Y. Tseng, *Light gauge boson interpretation for $(g - 2)_\mu$ and the $K_L \rightarrow \pi^0 + (\text{invisible})$ anomaly at the J-PARC KOTO experiment*, *JHEP* **04** (2020) 086, [2001.06572].
 - [31] J. N. Bahcall, *Solar neutrinos. I: Theoretical*, *Phys. Rev. Lett.* **12** (1964) 300–302.
 - [32] M. Boschini et al., *HelMod in the works: from direct observations to the local interstellar spectrum of cosmic-ray electrons*, *Astrophys. J.* **854** (2018) 94, [1801.04059].
 - [33] D. Banerjee et al., *Dark matter search in missing energy events with NA64*, *Phys. Rev. Lett.* **123** (2019) 121801, [1906.00176].
 - [34] J. Redondo, *Helioscope Bounds on Hidden Sector Photons*, *JCAP* **0807** (2008) 008, [0801.1527].
 - [35] S. Davidson, S. Hannestad and G. Raffelt, *Updated bounds on millicharged particles*, *JHEP* **05** (2000) 003, [hep-ph/0001179].
 - [36] G. Bellini et al., *Precision measurement of the ^7Be solar neutrino interaction rate in Borexino*, *Phys. Rev. Lett.* **107** (2011) 141302, [1104.1816].
 - [37] A. G. Beda, V. B. Brudanin, V. G. Egorov, D. V. Medvedev, V. S. Pogosov, M. V. Shirchenko et al., *Upper limit on the neutrino magnetic moment from three years of data from the GEMMA spectrometer*, 1005.2736.
 - [38] *Just pocket guide*, .
 - [39] N. F. Bell, G. Busoni and S. Robles, *Capture of Leptophilic Dark Matter in Neutron Stars*, *JCAP* **06** (2019) 054, [1904.09803].
 - [40] R. Garani, Y. Genolini and T. Hambye, *New Analysis of Neutron Star Constraints on Asymmetric Dark Matter*, *JCAP* **05** (2019) 035, [1812.08773].
 - [41] W.-Y. Keung, D. Marfatia and P.-Y. Tseng, *Heating neutron stars with GeV dark matter*, 2001.09140.
 - [42] S. D. McDermott, H.-B. Yu and K. M. Zurek, *Constraints on Scalar Asymmetric Dark Matter from Black Hole Formation in Neutron Stars*, *Phys. Rev.* **D85** (2012) 023519, [1103.5472].